Robotica (1999) volume 17, pp. 313–323. Printed in the United Kingdom © 1999 Cambridge University Press

Distributed ground/walking robot interaction

O. Bruneau and F.B. Ouezdou

Laboratoire de Robotique de Paris, CNRS-UPMC-UVSQ 10-12 Avenue de l'Europe, 78140 Vélizy (France)
e-mail: bruneau@robot.uvsq.fr

(Received in Final Form: September 17, 1998)

SUMMARY

Most of the time, the construction of legged robots is made in an empirical way and the optimization of the mechanical structure is seldom taken into account. In order to avoid spending time and money on the construction of many prototypes to test their performance, a CAD tool and a methodology seem to be necessary. In this way it will be possible to optimize on one hand the kinematic structure of the legs, on the other hand the gaits which will be used by the future robot. Thus, we have developed a methodology to design walking structures such as quadrupeds and bipeds, to simulate their dynamic behavior and analyse their performances. The feet/ground interaction is one of the major problem in the context of dynamic simulation for walking devices. Thus, we focus here about the phenomenon of contact. This paper describes a general model for dynamic simulation of contacts between a walking robot and ground. This model considers a force distribution and uses an analytical form for each force depending only on the known state of the robot system. The simulation includes all phenomena that may occur during the locomotion cycle: impact, transition from impact to contact, contact during support with static friction, transition from static to sliding friction, sliding friction and transition from sliding to static friction. Some examples are presented to show the use of this contact model for the simulation of the foot-ground interaction during a walking gait.

KEYWORDS: Legged robots; C.A.D. tool; Walking structure; Ground-feet interaction.

1. INTRODUCTION

Our work aims to optimize on one hand the mechanical structure of the legs, on the other hand the gaits which will be used by the future robot. Design of structures and gaits requires an iterative analysis tool able to simulate accurately the dynamic behavior of walking machines which are very large and complex systems. Therefore it is essential to improve the mechanical model of the system and its environment. Thus, it is necessary to model the feet/ground interaction during walking or running in order to simulate all the phases that may occur during the locomotion cycle. These phases are: single support phase, double support phase, n-support phase for n-legged robots, flight phase, impact, lift-off and landing.

We present in section 2, the two main models often used to simulate the feet/ground interaction phenomenon. The first one introduces intermittent kinematic joints implying kinematic constraints which keep the feet on the support surface. The second model introduces spring-damper elements between the feet and ground. An analysis of the two models, showing the limits of each one, leads us to propose a new contact model. This model, based on a distributed contact force depending on the known state of the system, is presented in section 3. In section 4, some examples of contact simulation of walking biped are presented: impact, contact, sliding and transition phases between these phenomena. Furthermore, limits of the model and further developments are given.

2. CONTACT MODELS

In major recent works dealing with locomotion and feet-ground interaction, two main models are often used for the walking robots simulation. The first one uses kinematic constraints and Lagrange multipliers which give the contact reaction forces. The second one uses spring-damper elements between the feet and ground mainly to simulate compliance. We describe these two models in the following subsections and show their advantages and deficiencies.

2.1 Kinematic constraints

In this first approach, the system of motion equations is complemented by constraint equations defining the conditions for fixation of one or several feet on the ground.[1] The contact between feet and support is assumed to be punctual: either the contact is really a point, or massless feet stay parallel to the floor during the motion. The dynamic equations of motion are established by considering intermittent contacts leading to a time-varying number of closed loops. The introduction of perfect kinematic joints at the contact points implies kinematic constraints which attempt to keep the feet on the support surface. The constraint equations (specified as velocity functions) are multiplied by Lagrange multipliers and the coefficients of each velocity variable represent constraint forces acting on the corresponding degrees of freedom. Here the constraint forces are the ground reaction force acting on the joint between feet and ground. The whole system of equations is the following:

$$M(q)\ddot{q}+S(q,\dot{q})+G(q)=\tau+D(q)^{t}\Gamma \quad (1)$$

$$D(q)\ddot{q}+E(q,\dot{q})=0 \quad (2)$$

Equation (2) is obtained by time derivation of:

$$D(q)\dot{q}=0 \quad (3)$$

https://doi.org/10.1017/S0263574799001290 Published online by Cambridge University Press

where $M(q)$ is the inertial matrix, $S(q, \dot{q})$ the Coriolis and centrifuge vector, $G(q)$ the gravity terms, τ the actuation vector, $D(q)$ the kinematics constraints matrix depending on the location of contacts and Γ Lagrange multipliers. In the case of existing an active ankle, a torque[1,2] is added in the actuation vector τ. The impacts introduced by feet landing are assumed to be perfectly inelastic. They are modeled by impulsive forces implying a discontinuity in some components of generalized velocities. Considering that the impact occurs in an infinitesimally short time period, all the terms having finite amplitude in the equations of motion (gravity forces, actuation and friction forces) do not contribute to the impact phenomenon. The equations to model the impact are derived using Lagrange equations for impulsive forces[3,4] which lead to:

$$M(q)\dot{q}^{+} - M(q)\dot{q}^{-} = I_{v} \tag{4}$$

where $\dot{q}^{+}$ and $\dot{q}^{-}$ are, respectively, the joint velocity vectors just before and just after impact, and I_v is the vector of impulse applied to the joints during impact, including impact forces and joint impulsive moments. Several studies have recently made significant advances concerning dynamics of systems submitted to unilateral constraints.[5–7] This can be shown to be a linear complementary problem (LCP). A survey of recent contributions in this field can be found in reference [8].

2.2 Spring-damper model

The second approach uses spring-dampers elements between the feet and the ground for modeling contact.[9,10] The simplest contact model used is a spring-damper parallel combination between the feet and the ground at the contact point. The interaction force for the contacting objects is given by the equation:

$$f_{y} = -k_{y}y - \mu_{y}\dot{y} \tag{5}$$

where y is the penetration depth, μ_y is the damping coefficient and k_y is a stiffness constant (Figure 1). This model can be used for the two others axis (x, z). The force applied on the j^{th} contacting foot can be written in a reference frame (R, O, $\vec{x}$, $\vec{y}$, $\vec{z}$) as:

$$f_{j} = [f_{x_j}, f_{y_j}, f_{z_j}]^{t} \tag{6}$$

At each instant, there are n_{ps} legs in contact with the ground. The vector of reaction force is:

$$\hat{f} = [f_{1}, f_{2}, \ldots, f_{n_{ps}}]^{t} \tag{7}$$

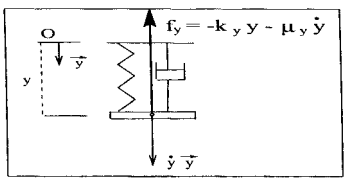

Fig. 1. Spring-damper model.

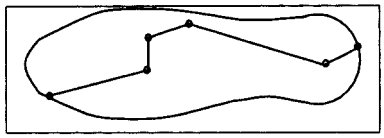

Fig. 2. Pressure center evolution during walking.

The system of equations becomes:

$$M(q)\ddot{q} + S(q, \dot{q}) + G(q) = \tau + D(q)^{t}\hat{f} \tag{8}$$

2.3 Discussion about the two approaches

2.3.1 A single fixed contact point. Usually, in the first approach, the chosen joint to model the contact is a punctual contact without sliding (i.e. an infinite friction coefficient) with the unilateral contact assumption. This kind of choice is consistent with theory of rigid solids dynamics but leads to some remarks. At first, the assumption of a single contact point which is fixed during a given support phase is not so realistic. Indeed, if we observe the ground reaction with a Footprint System[11] for a human being during walking, the contact domain is a surface and not a point. It can be supposed that the same phenomenon occurs for an efficient biped robot with feet. Furthermore, the contact area is varying versus time and the pressure center is moving under the foot during the period of support (Figure 2).[2] Finally, just one contact point under each foot, with a perfect joint between foot and ground, implies that the ground do not apply any torque to the foot. However real ground exerts moments on each foot of a real walking device.[11]

The second approach uses a model that presents some deficiencies.[13] At first, the contact force is discontinuous at the moment of impact because of the damping term $-\mu\dot{y}$, whereas the interaction forces physically should start at zero and increase over time. Secondly just before separation of the objects, $\dot{y}$ will be negative which implies an attractive force tending to hold the objects together. A classical solution is to set this force to zero when separation arises. This approach is often used with the single point contact assumption which presents some limits for modeling the feet/ground interaction. However, this approach can be extended to a set of contact points as it will be proposed in section 3.

2.3.2 Rigid or compliant contact? For the two approaches, the wrench system is the same at each leg/ground contact point j ($1 \le j \le n_{ps}$). The wrench system is reduced to a single force which has three components:

$$\hat{W}_{j} = [0, 0, 0, f_{xj}, f_{yj}, f_{zj}] \tag{9}$$

However, the twist system is not the same. In the first approach, the joint at the contact point is supposed to be a unilateral contact. Thus the twist system is reduced to three angular velocities components (Figure 3):

$$\hat{T}_{j} = [\omega_{j}, \omega_{y_j}, \omega_{z_j}, 0, 0, 0] \tag{10}$$

https://doi.org/10.1017/S0263574799001290 Published online by Cambridge University Press

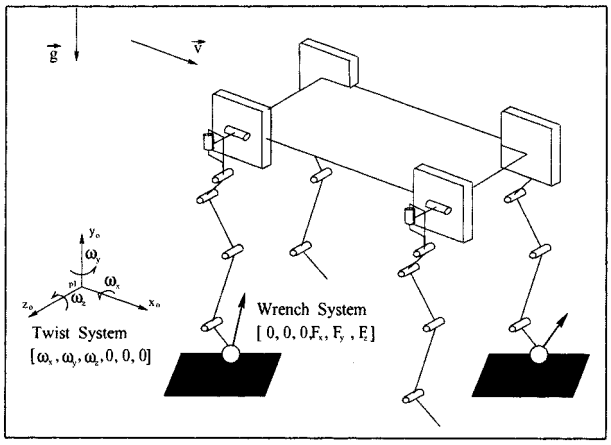

Fig. 3. Quadruped example with spherical joint as contact model.

In the first approach, the feet and the ground are assumed to be rigid solids. This assumption is not always verified for a real robot walking in a real environment. So, a parametric contact model has to be considered, which permits to simulate both contact between rigid bodies and contact between elastic ones. Concerning this remark, the second approach is more realistic, namely to simulate compliance between the foot and the ground and visco-elastic effects during collision.

In the second approach, the twist system has six components: three linear velocities associated to small amplitude translational motions due to contact compliance and three angular velocities associated to the rotations around the contact point. The twist system is the following (see Figure 4):

$$\hat{T}_j = [\omega_{x_j}, \omega_{y_j}, \omega_{z_j}, \epsilon v_{x_j}, \epsilon v_{y_j}, \epsilon v_{z_j}] \tag{11}$$

The existence of components of linear velocities in the twist system shows that small deformations may exist for the two objects in contact. The stiffness constant can be chosen large to simulate a contact between near rigid bodies and small to simulate a contact between elastic bodies. The damping coefficient can be chosen large if there is a lot of energy loss caused by the material damping of the bodies.

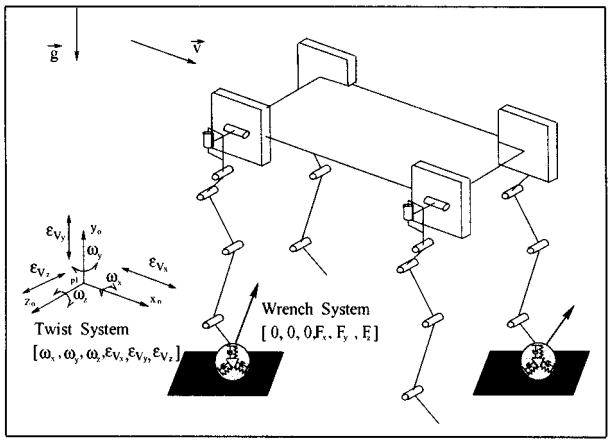

Fig. 4. Quadruped example with a 3D spring-damper as contact model.

2.3.3 Calculation of the ground reaction. In the first approach, the ground reaction forces are unknown and are calculated thanks to the Lagrange multipliers. Two kinds of dynamic formulations can be addressed for the legged locomotion systems: the direct and the inverse problems. The direct dynamic model can be addressed as computing the resulting motion due to a given set of joints forces/ torques. However, for a legged robots, it is necessary to determine also the contact forces between the feet and the ground. Hence, we have to establish a *hybrid* form of usual known direct dynamic model (i.e. for manipulators). This hybrid model yields to compute the resulting motion and the contact forces. The solution of this problem exists and is unique. The inverse problem consists on computing necessary active forces-torques for a desired law of motion of the walking machine platform. We have also to compute the contact forces f which depend on the active joint torques. The inverse dynamic model of legged robot can be addressed as following:

$$(\tau, f) = \widetilde{\mathcal{G}} (\ddot{q}, \dot{q}, q) \tag{12}$$

In order to express equation (12), we assume that the platform acceleration is already known. In general, we have more unknowns than equations which leads to an infinite number of solutions. In order to find a particular solution, we can solve an optimisation problem. Many objective functions can be used to compute an optimal solution such as the energy consumption or the contact force balancing.

In the second approach, one assumption is made and remains always the same: the foot/ground interaction is submitted to a behavior law where the force depends explicitely on the relative motions of the two contacting objects. So, in this case, no additional assumptions is required to calculate the reaction force even if there are more than one foot in contact with ground. The generalized coordinates and velocities are calculated on each step of the integration procedure from the solution of equations of motion and the interaction forces are directly calculated because they depend only on the known state of the walking machine. Finally, this second approach avoids the system reconfiguration required at change of support transitions.

2.4 Choice of the model

According to last subsection, the spring-damper approach is chosen in order to simulate the compliance between the robot and its environment. However, it is not so realistic to choose just one fixed point. Furthermore, a specific model must be used for the tangential forces during contact with sliding. Moreover, the simple spring/damper parallel combination has not all the properties required to simulate the normal ground reaction and some modifications of this model must be made. However the contact model must stay rather simple. In fact, a compromise must be found between complexity of the model and realism. So we present in the next section a model which consider a force distribution and uses an analytical form for each force depending only on the known state of the walking robot.

https://doi.org/10.1017/S0263574799001290 Published online by Cambridge University Press

3. DISTRIBUTED CONTACT MODEL

3.1 Contact behavior model

3.1.1 Contact without sliding. The best known force model for the contact simulation between two objects is a linear spring/damper parallel combination between the objects at the contact point (see Eq. 5, Figure 1).

Another model was developed by Hertz in 1881 based on the theory of elasticity[14] giving the interaction force:

$$f_y = -k_y y^{\alpha} \text{ where } \alpha = 3/2 \tag{13}$$

The major drawback of this model is that no energy is dissipated during the process of impact. We can also add a linear damping function and use the Kelvin-Voigt model[14]:

$$f_y = -k_y y^{\alpha} - \mu_y \dot{y} \tag{14}$$

But we will have the same problems as the model with the linear spring-damper parallel combination given by equation (5) as described by Marhefka.[13] A hysteresis form for the damping coefficient was proposed by Hunt[15] and used by Marhefka:[13]

$$f_y = -k_y y^{\alpha} - \mu_y y^{\alpha} \dot{y} \tag{15}$$

where α is a rational number. With this model (Eq. 15), the energy loss is caused by the material damping of the bodies which dissipates energy in the form of heat. Furthermore, this model seems to be physically meaningful: greater is the depth, larger is the contact surface of the two bodies and more important is the damping force. The contact point assumption presents some limits for modeling the foot/ground interaction. Thus, a distributed contact model is chosen by placing N points P_i (called the testing points) on the lower part of the feet (Figure 5). Just when they touch the ground, on each contact point P_{ci}, we can define a tangent plane (π) to the ground and its associated local frame $\Re_{ci}(P_{ci}, \vec{X}_{ci}, \vec{Y}_{ci}, \vec{Z}_{ci})$ where $\vec{Y}_{ci}$ is the normal to (π), $(\vec{X}_{ci}, \vec{Z}_{ci}) \in \pi^2$ and $\vec{X}_{ci}.\vec{Z}_{ci} = 0$. The coordinates of a point P_i (x_i, y_i, z_i) in this frame represent the foot/ground geometric interference (Figure 6). In respect to frame $\mathbf{R}_{ci}$ the normal component of the contact force in $\vec{Y}_{ci}$ direction is given by:

$$f^*_{n_i} = k_n(-y_i)^{\alpha} - \mu_n(-y_i)^{\beta}\dot{y}_i \tag{16}$$

where k_n and μ_n are the generalized stiffness and damping coefficients for normal direction. The model considers different exponent terms α and β for the stiffness force and the damping force in order to choose these parameters

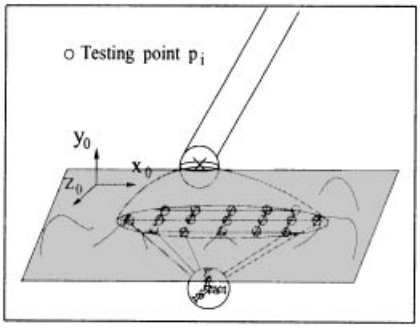

Fig. 5. Location of the testing points.

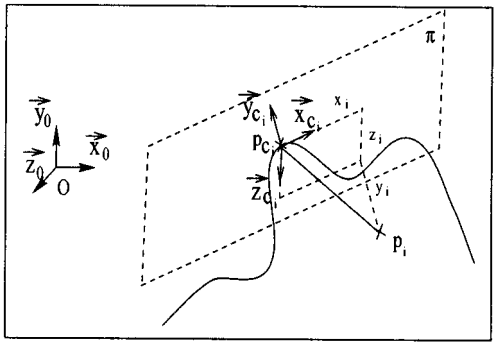

Fig. 6. Geometric interference.

separately as functions of the contacting bodies properties. Parameters α and β are determined through a parametric simulation analysis. Tangential force $f^*_{t_i}$ can be expressed by its two components in $\vec{X}_{ci}$ and $\vec{Z}_{ci}$ directions which are friction forces that occur on each point. The following model is used to express these components:

$$f^*_{x_i} = -k_t x_i - \mu_t \dot{x}_i \tag{17}$$

$$f^*_{z_i} = -k_t z_i - \mu_t \dot{z}_i \tag{18}$$

where k_t, and μ_t are generalized stiffness and damping coefficients for tangential forces. The tangential force magnitude can be then expressed as:

$$f^*_{t_i} = \sqrt{f^{*2}_{x_i} + f^{*2}_{z_i}} \tag{19}$$

3.1.2 Contact with sliding. In a lot of simulation tools for walking robots, sliding is not taken into account. Generally the robot is controlled in order to avoid sliding by imposing to keep the force in the static friction cone, and, as soon as the tangential force reaches the sliding limit, simulation is stopped. Then, if we want to bring simulation closer to reality, it is required to simulate sliding. It would be then possible to study control strategies or to design feet in order to avoid the collapse of the robot. The modeling of dynamic sliding friction was very large investigated. A general friction model was proposed by Canudas et al.[16] This model combines the stiction behavior, i.e., the Dahl effect, with arbitrary steady-state friction characteristics which can include Stribeck effect.[17] We present here a basic model which neglect the Stribeck effect and attempt to model the sliding phenomenon of a legged robot during walking. This model is based on discretised contact surface that allows us to take into account the sliding effects at local and global levels.

Let λ_s be the static Coulomb friction coefficient, which depends on the nature of the surfaces in contact. While $f^*_{t_i} < \lambda_s f^*_{x_i}$ there is no sliding and equations (16, 17, 18) are used to compute the contact forces. When $f^*_{t_i}$ becomes equal to $\lambda_s f^*_{n_i}$, sliding begins. Let t_i be a vector given by the ratio of the tangential force $(f^*_{t_i})^s$ components just at the beginning of sliding called $(f^*_{x_i})^s$ and $(f^*_{z_i})^s$. This unit vector is determined by its cosine directors given as follows:

$$\vec{t}_i.\vec{X}_{ci} = \frac{(f^*_{x_i})^s}{(f^*_{t_i})^s} = \cos(\theta_i) \text{ and } \vec{t}_i.\vec{Z}_{ci} = \frac{(f^*_{z_i})^s}{(f^*_{t_i})^s} = \sin(\theta_i) \tag{20}$$

https://doi.org/10.1017/S0263574799001290 Published online by Cambridge University Press

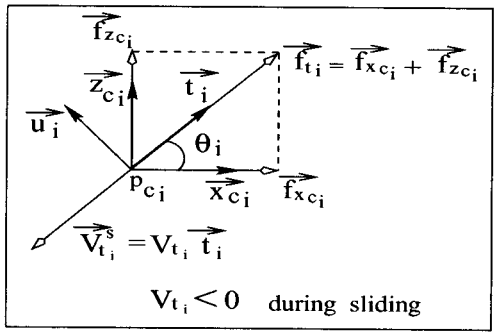

Fig. 7. Sliding velocity and direction.

During sliding, an idealized model of dynamic friction is often used to determine the tangential force $\vec{f}^s_{t_i}$ applied on an object contacting a surface as function of the normal force $\vec{f}^s_{n_i}$.

$$\vec{f}^s_{t_i} = \lambda_d \|\vec{f}^s_{n_i}\|(-Sgn\,(V_{t_i}))\vec{t}_i \tag{21}$$

Where $\vec{V}_{t_i} = V_{t_i}\vec{f}_i$ is the velocity of the object relative to the ground during sliding ($V_{t_i} < 0$) (Figure 7). λ_d is the sliding friction coefficient which depends on the nature of the surfaces in contact and on their lubrication conditions. The major drawback of this model (Eq. 21) is that, in the case of persistent contact (no detachment), the transition from sliding to adherence will be impossible. Indeed, the tangential forces depend only on the normal ones. To stop sliding, the tangential forces have to go to zero requiring a normal force equal to zero also (detachment). To improve this model, the tangential force should depend also on tangential velocity in order to take into account tangential viscous damping. So, a new expression of $\vec{f}^s_{t_i}$ is proposed as following:

$$\vec{f}^s_{t_i} = (\lambda_d \|\vec{f}^s_{n_i}\|(-Sgn(V_{t_i})) - \mu^s_t \,|\, V_{t_i} \,|)\vec{t}_i \tag{22}$$

where μ^s_t is a tangential viscous damping during the sliding. Another major problem is to determine what is the exact direction of sliding $\vec{t}_i$ in order to know exactly the values of $f^s_{x_i}$ and $f^s_{z_i}$ in respect to $\mathbf{R}_{ci}$. We assume that the relative velocity of point P_{ci} during the entire phase of sliding has the opposite direction to the tangential force just before sliding ($\vec{t}_i$) and this direction does not change during sliding. In this case, the force on each contacting point in respect to $\mathbf{R}_{ci}$ is given as follows:

$$f^s_i = [f^s_{x_i}, f^s_{n_i}, f^s_{z_i}]^t \tag{23}$$

The normal component is given in the same way by equation (16):

$$f^s_{n_i} = k_n(-y_i)^\alpha - \mu_n(-y_i)^\beta \dot{y}_i \tag{24}$$

Using equations (20) and (22), the tangential forces during sliding in respect to $\mathbf{R}_{c_i}$ are:

$$f^s_{x_i} = (\lambda_d f^s_{n_i} - \mu^s_t \dot{x}_i)\cos(\theta_i) \tag{25}$$

$$f^s_{z_i} = (\lambda_d f^s_{n_i} - \mu^s_t \dot{z}_i)\sin(\theta_i) \tag{26}$$

The problem raised by equations (25) and (26) is that the foot discontinuously switches from being stationary to sliding and tangential forces are then discontinuous. To avoid this problem, a transition model during a short period can be used. A linear interpolation of the tangential force over time from the no sliding model (Eq. 17 and 18) to the sliding one (Eq. 25 and 26) may be carried out as following:

$$f^{*s}_{u_i} = f^*_{u_i} + (f^s_{u_i} - f^*_{u_i})\frac{t - t^{*s}_i}{T_{*s}}\, u \in \{x, z\} \tag{27}$$

where t is time and T_{*s} is parameter giving the duration of the transition and depending on the physical properties of surfaces in contact. t^{*s}_i is the instant of the begining of sliding at each testing point determined by using the following condition:

$$f^*_{t_i} = \lambda_s f^*_{n_i} \tag{28}$$

In the same way, we have to establish a transition model from the sliding phase to adherence phase. A linear interpolation of the tangential forces over time is also carried out:

$$f^{s*}_{u_i} = f^s_{u_i} + (f^*_{u_i} - f^s_{u_i})\frac{t - t^{s*}_i}{T_{s*}}\, u \in \{x, z\} \tag{29}$$

where T_{s*} is parameter giving the duration of the transition and t^{s*}_i is determined using the following condition on the sliding velocity:

$$V_{t_i} \geq 0 \tag{30}$$

We discuss now in more details the distributed contact force including contact detection, the use of the model in different cases such as impact, static friction, sliding friction and transition phases between these phenomena.

3.2 Distributed contact force

3.2.1 Number of testing points. The testing points, on which forces are applied, are placed on the lower part of the feet. Two contact points in the 2D-case (Figure 8) or four contact points in the 3D-case are sufficient to avoid that the foot sinks into the ground. However these models imply a non-progressive contact between the feet and the ground. For instance, during walking with a compliant contact: the heel touches the ground; after that, the entire foot surface progressively comes into contact with it; finally the toes touch it. With the model given in (Figure 8) for instance, there is one contact point when the heel touches the ground and the next contact arises just when the toes come into

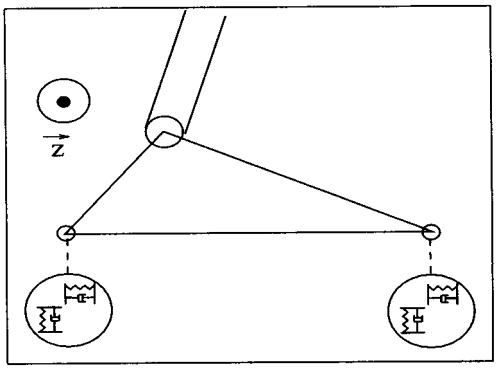

Fig. 8. Two contact points.

https://doi.org/10.1017/S0263574799001290 Published online by Cambridge University Press

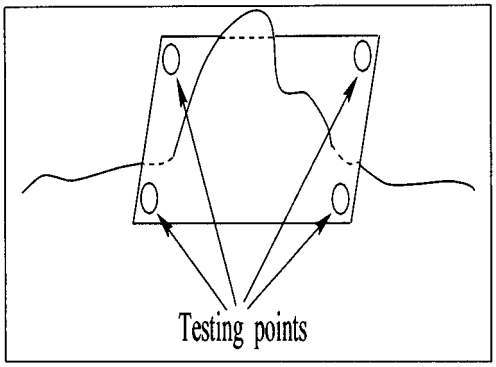

Fig. 9. No contact detection.

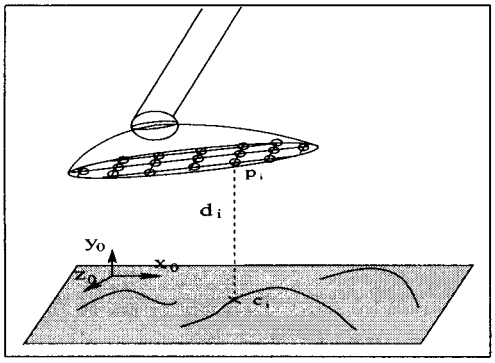

Fig. 10. Contact detection.

contact with the ground. The toes have then a large velocity (compared to the velocity they would have if the contact would be progressive). A large force is also applied on the toes only and this force has not a real physical meaning. On the contrary to this approach, the reaction force must be progressively applied and distributed on the entire foot. Moreover these models are unuseful if the support surface have imperfections due to stones or bumps in the ground. For instance in the case of an irregular ground, if we suppose that we have only four testing points on the four edges of each foot, the irregularities can geometrically interfere with the foot, without taking into account them in the contact mechanics (Figure 9). These remarks lead us to propose a model where the testing points cover the entire lower part of the feet. They form a grid with regular spaces between them. A larger number of testing points implies a more progressive interaction and the reaction forces are better distributed. Naturally, a larger number of testing points is required if the ground is very irregular. Thanks to this model, the contact domain can be a point, a line or a surface depending on the geometry of the two objects in contact.

3.2.2 Contact detection. The contact detection is generally treated as a geometric interference problem depending on the spatial relationship of objects. However impact/contact response is a dynamic problem which involves predicting behavior according to physical laws. A lot of methods exist for detecting the contacts between a moving object A and a fixed base B. The objects are modeled as a general polyhedron composed by set of vertices, edges, and faces (Boundary Representations) or the surface of the objects are represented by analytical functions (Analytical Surface Representation) or by volumetric cylinders or spheres organised in hierarchical tree-structure (Constructive Solid Geometry Representations).[18] All these methods consist of iterative procedures which aim to find the nearest point between A and B and then to simulate contact in this point. Instead of determining at each time step, which is the nearest point to the ground surface, we choose to cover the lower part of the feet by a predefined grid M_s of N testing points p_i. All these points are orthogonally projected to the ground. These projections are represented by N points c_i and the distance $d_i = \| \overrightarrow{p_i c_i} \|$ is checked. As soon as $d_i = 0$, a three-dimensional force is applied on the concerning testing points p_i. The algorithm complexity is reduced because the points on which the forces will be applied are known in advance without search procedures of the nearest point to the ground. If we summarize: all the testing points have thus an identical status: a force is applied on p_i as soon as $d_i = 0$ (Figure 10).

3.2.3 Macroscopic and local contact. We have to consider contact phenomena at two levels: macroscopic and local contact. The local one depends on the behavior of one testing point as exposed in the previous subsections. A general form of this local model can be expressed using a boolean variable g_{s_i} initialised to 0 and taking a value of 1 only when sliding appears. The sliding condition can be formulated locally as: *Sliding occurs when* $f^*_{t_i}$ *becomes equal to* $\lambda_s f^*_{n_i}$ *and stops when* $V_{t_i} \geq 0$.

In respect to R_{ci}, the force applied on each testing point can be expressed using g_{s_i}.

The normal force f_{n_i} is the same during all phases and can be computed using either Equation (16) or Equation (24):

$$f_{n_i} = f^*_{n_i} = f^s_{n_i} \tag{31}$$

The tangential forces on each testing point have the following general form:

$$\begin{aligned} f_{u_i} = (1 - g_{s_i})\{(1 - g_i^{s*}) f^*_{u_i} + g_i^{s*} f^s_{u_i *}\} \\ + g_{s_i}\{(1 - g_i^{*s}) f^s_{u_i} + g_i^{*s} f^{*s}_{u_i}\} \quad u \in \{x, z\} \end{aligned} \tag{32}$$

where g_i^{s*} and g_i^{*s} are Boolean determined as following:

$$g_i^{s*} = \begin{cases} 1 \text{ if } t_i^{s*} \leq t \leq t_i^{s*} + T_{s*} \\ 0 \text{ otherwise} \end{cases} \tag{33}$$

$$g_i^{*s} = \begin{cases} 1 \text{ if } t_i^{*s} \leq t \leq t_i^{*s} + T_{*s} \\ 0 \text{ otherwise} \end{cases} \tag{34}$$

The forces f^*_{ui} are given by relations (17 and 18) and f^s_{ui} are determined using equations (25 and 26). The transition forces $f^{s*}_{u\,i}$ and $f^{*s}_{u\,i}$ are given by equations (27 and 29).

However, the macroscopic phenomenon has to consider the global behavior of the feet on the ground and the local sliding condition should be changed on a global one. Let $\vec{f}_{x_i}$,

https://doi.org/10.1017/S0263574799001290 Published online by Cambridge University Press

$\vec{f}_{y_i}$ and $\vec{f}_{z_i}$ be the forces acting upon each testing point with respect to the reference frame. The sum of all the forces applied on each contacting foot $j (j = 1, n_{ps})$ in respect to this frame are:

$$\vec{F}_{xj} = \sum_{i=1}^{N} \vec{f}_{x_i} \quad \vec{F}_{yj} = \sum_{i=1}^{N} \vec{f}_{y_i} \quad \vec{F}_{zj} = \sum_{i=1}^{N} \vec{f}_{z_i} \tag{35}$$

If we assume that the foot contact surface and the ground are planar surfaces with $\vec{y}$ as normal vector, the normal and tangential forces can be written as following:

$$\| \vec{F}_{nj} \| = \| \vec{F}_{yj} \| \quad \| \vec{F}_{tj} \| = \sqrt{\| \vec{F}_{xj} \|^2 + \| \vec{F}_{zj} \|^2} \tag{36}$$

Let λ_g be the ratio of the tangential and normal contact forces applied on the foot j given by this relation:

$$\lambda_g = \frac{\| \vec{F}_{tj} \|}{\| \vec{F}_{nj} \|} \tag{37}$$

We notice that for some configurations, the sliding of the foot begins before λ_g reaches the friction coefficient limit λ_s. This phenomenon is due to the fact that the testing points do not slide exactly at the same time. This is realistic fact, but the static friction coefficient λ_s is a measured parameter valid at the macroscopic scale (i.e. Coulomb law).

So, the local sliding condition "*Sliding occurs when* f_{ti}^* *becomes equal to* $\lambda_s f_{ni}^*$" must be changed by "*Sliding occurs when* $\| \vec{F}_{tj} \|$ becomes equal to $_s \| F_{tmj} \|$". This new sliding condition induces the fact that all testing points begin to slide at the same instant t^{*s}:

$$t^{*s} = t_i^{*s} \quad 1 \leqslant i \leqslant N \tag{38}$$

This yields to:

$$g_i^{*s} = g^{*s} \quad 1 \leqslant i \leqslant N \tag{39}$$

To take into account the macroscopic and local phenomena, the set of N variables g_{s_i} has to be determined by observing these two conditions:

cond. 1. $\| \vec{F}_{tj} \| < \lambda_s \| \vec{F}_{nj} \|$ (macroscopic)

cond. 2. $V_{ti} \geq 0$ (local)

The following algorithm is used to compute g_{s_i} for each testing point:

$$g_{s_i} = \begin{cases} 0 & \text{while (cond.1 or cond.2)} \\ 1 & \text{otherwise.} \end{cases} \tag{40}$$

In conclusion, the N variables g_{s_i} switch from 0 to 1 at the same time (global) and from 1 to 0 individually (local) which allows us to simulate all the phases during the walk. The forces applied on the testing points imply a moment acting upon each foot. We can calculate this moment in respect to the joint center that attach the legs to the feet for instance. Let (bx_j, by_j, bz_j) (with j = 1, 2 for a biped, or j = 1, ... , 4 for a quadruped) be the coordinates of this point B_j in a frame attached to the ground (see Figure 11),

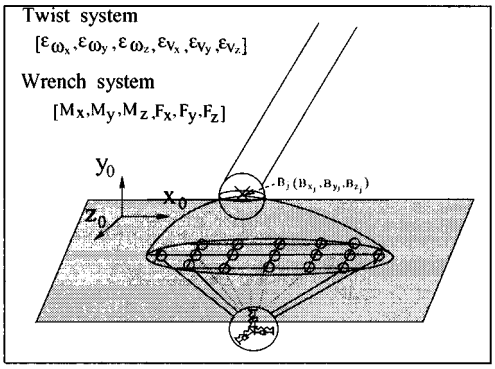

Fig. 11. Foot/ground interaction.

and (px_i, py_i, pz_i) (with i = 1 to N for each foot) the coordinates of the N testing points p_i in the same frame, the resulting moment of forces in respect to B_j is then:

$$\vec{M}_j = \sum_{i=1}^{N} \overrightarrow{B_j p_i} \wedge (\vec{f}_{x_i} + \vec{f}_{y_i} + \vec{f}_{z_i}) \tag{41}$$

So, the proposed model leads to a moment acting upon each foot created by the set of the three-dimensional forces applied on the testing points. Thus it is more realistic than the unique contact point assumption, where no moment appears at the contact point.

Furthermore the contact area and the pressure center can vary versus time, this phenomenon is near to reality and specially in the case of a biped robot with large feet.

Moreover, parameters such as stiffness (k_n, k_t), damping (μ_n, μ_t) and exponents (α, β) introduce the notions of compliant contact. Then the feet and the ground are not considered as perfectly rigid solids. The parameters $(k_n, k_t, \mu_n, \mu_t, \alpha, \beta)$ permit to change the physical nature of the contacting solids. Finally, during contact without sliding, phenomena such as compliance, friction and impulsive impacts are simulated by the same model of three-dimensional forces applied on each testing point. The motion equations reconfiguration due to intermittent closed chains are avoided.

4. RESULTS AND DISCUSSION

4.1 Application

We have used this contact model for a walking biped robot which has a total weight of 75 kg. The general model consists of a trunk, a pelvis, two arms, two upper legs, two lower legs and two feet. There are three rotational degrees of freedom per joint, except for the pelvis which has six degrees of freedom. This is the model proposed by Hanavan.[19] This robot is a 3D-device, but for convenience, because of equilibrium problems in the frontal plane, we impose that the motions stay always in the same plane defined by gravity $(\vec{y})$ and the main direction of robot displacement $(\vec{x})$. We use here the same technique as Raibert[10] for its planar running bipeds. In fact, we lock a lot of degrees of freedom: we keep only one degree of freedom per joint (the rotation around $\vec{z}$). There are two degrees of

https://doi.org/10.1017/S0263574799001290 Published online by Cambridge University Press

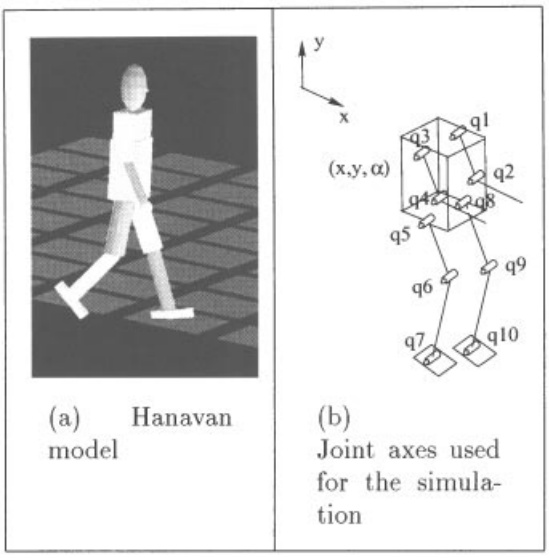

Fig. 12. Walking biped model and parameters used for the simulation.
a) Hanavan model
b) Joint axes used for the simulation

freedom for each arm and three for each leg. Concerning the pelvis we keep three degrees of freedom (angular position γ, cartesian position x, y) and we assume that the trunk is rigidly connected to the pelvis. Finally we obtain the model given on Figure 12(b). We have covered the lower part of each foot by a predefined set of $N = 18$ testing points where forces can be applied. By imposing a maximum geometric normal interference of 1 cm and a maximum tangential interference of 1 mm between foot and ground during a nominal walking gait, we have found the following values for the model parameters through an iterative simulation analysis:

k_n	μ_n	k_t	μ_t	α	β	μ_s^t	T_{*s}	T_{s*}
9950	450	90	950	1.2	0.02	1	0.01	0.01

Some examples of a walking biped simulations illustrate the use of the proposed foot/ground model contact to carry out impact, contact during support phase and sliding with transitions from adherence to sliding and from sliding to adherence.

4.1.1 Impact. By using the non linear spring-damper parallel combination for each testing point, the contact forces vary continuously over time during impact and contact. For instance, if we let fall down vertically the biped structure from a height of 30 cm, the total ground reaction grows up from 0 to the maximum and decreases continuously from this maximum to the weight of the structure. After the maximum of normal impulse the ground reaction reaches 110% of the weight in 0.012 s (Figure 13).

4.1.2 Contact during support phase. We have tested the model during a dynamic walking gait of an anthopomorphic

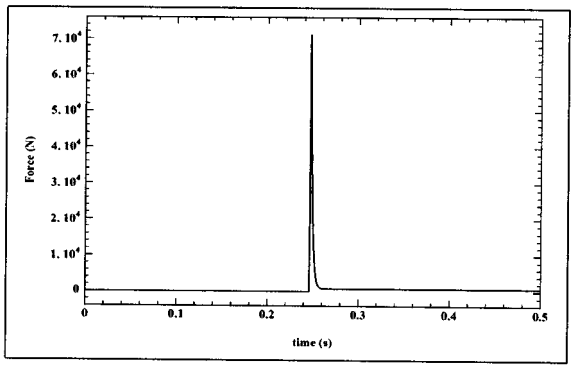

Fig. 13. Normal impulse.

biped robot with an average speed of 1.35 *m*/*s*. The robot has approximately the same mass distribution and geometry as a human and its weight is 75 kg. The motions of all the links are defined as functions of time and approximate the recorded motions of a real human by the means of polynoms.[20]

We obtain some interesting results (Figure 14 and 15). The curves with dotted lines are data of ground reaction (sagittal and normal) recorded for the human. Solid curves are results of our distributed contact model.

At first, we see that the forces vary continuously from impact (at low velocity) to contact during the walking gait. Secondly, during contact, the normal resultant force curve has the same shape as the recorded one: there is two maximas over the line of the weight and a minima between

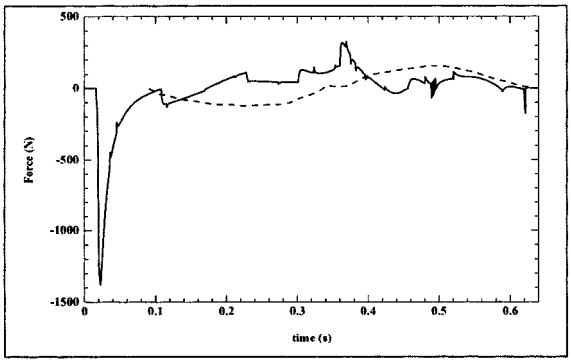

Fig. 14. Tangential force.

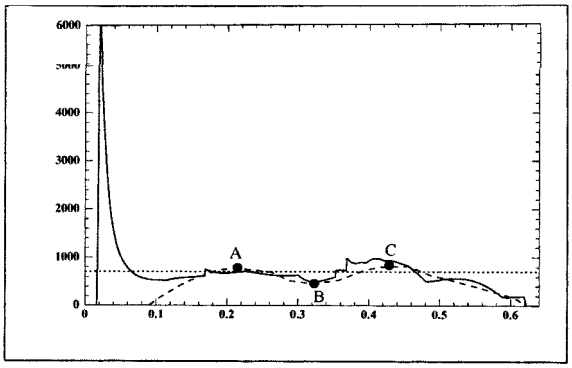

Fig. 15. Normal force.

https://doi.org/10.1017/S0263574799001290 Published online by Cambridge University Press

these two maximas under this line. Furthermore, all phases of the locomotion cycle are simulated: end of single support phase (Figure 16(a) and 16(b) (zoom of 16(a))), double support phase (Figure 16(c)), lift-off of the foot (Figure 16(d)), contact of the entire foot just after heel-touch (Figure 16(e)), middle of the single support phase (Figure 16(f)).

4.1.3 Sliding. A simple situation is simulated during 0.7 seconds to demonstrate the capabilities of the proposed model. The biped stands up with spread legs and a horizontal force is applied on each ankle (Figure 17(a) and a zoom given by 17(b)). The total pulling force versus time is given by broken lines on Figure (18). As the pulling force grows up, the biped goes from adherence to sliding at instant $t^{*s}=0.156\ s$; When the pulling force goes to zero, the sliding phenomenon remains for a short period and stops at instant $t^{s}*=0.496\ s$ (in this case, this instant is the same for all testing points $t^{s}*=t_i^{s}*\ \ 1 \le i \le N=18$). The total normal force F_n and the tangential contact forces F_t are also shown on Figure (18). We distinguish several phases that are given on Figures (19(a) to 19(f)).

Phase a: Steady state
Pulling and tangential forces are equal to zero and the biped is fixed.

Phase b: Adherence
The pulling force grows up inducing an increase of tangential forces and then of the ratio λ_g (Eq. 37).

Phase c: Adherence to sliding
The ratio λ_g reaches λ_s (static friction coefficient, equal to 0.7) and the biped begins sliding. The transition is varying continuously according to Equation (27).

Phase d: Sliding
The ratio λ_g is slightly greater than the dynamic friction coefficient λ_d (=0.4) due to the viscous damping introduced by Equation (22). We notice that the ratio λ_g is varying inversely proportional to the sliding velocity (see Figure 20).

Phase e: Sliding to adherence
The sliding velocity sign of all testing points changes at the same time $t^{s}*$ leading to going into the transition phase described by Equation (29). The tangential force goes to zero including the decreasing of ratio λ_g from λ_d to zero.

Phase a: New steady state
The biped reaches then a new steady state where it is fixed again.

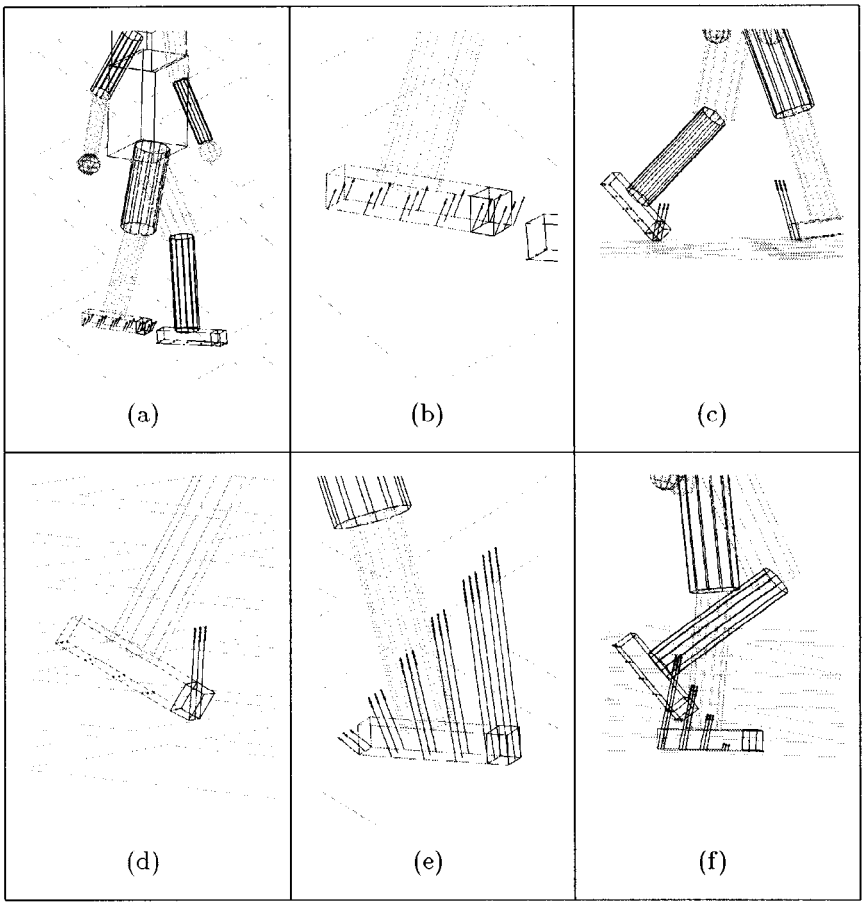

Fig. 16. Differents contact phases.

https://doi.org/10.1017/S0263574799001290 Published online by Cambridge University Press

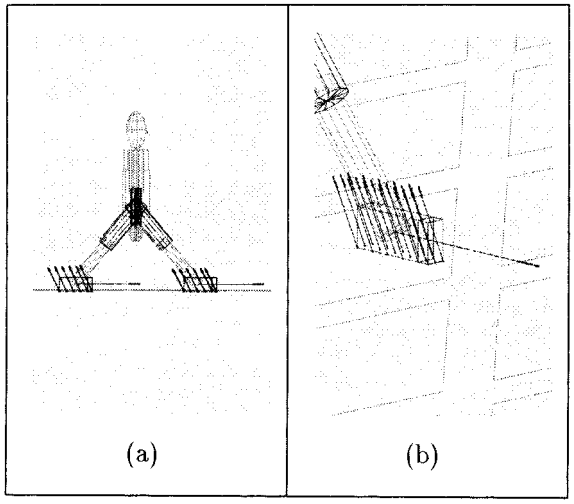

Fig. 17. Sliding simulation.

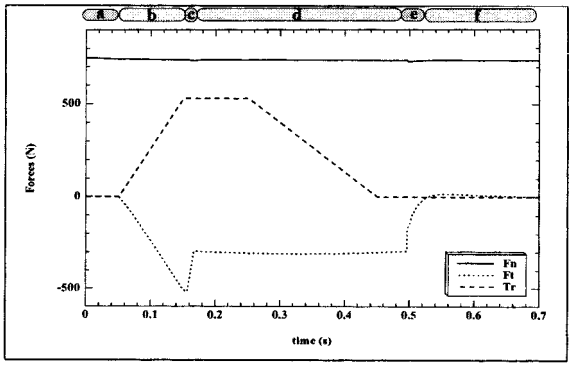

Fig. 18. Normal, tangential and pulling forces.

4.2 Further developments

We have compared the standard recorded ground reaction for a walking human and the results of our simulation. The curves obtained by simulation are not completely smooth during support phase (Figure 14): on the one hand, all the limbs are rigid links (except for the feet) connected by perfect joints and thus reactions are not so smooth as for a human; on the other hand, an accurate study must be made to know what is the ideal number of testing points required to be closer to the standard recorded ground reaction.

The major difficulty arises for the choice of the parameters: k_n, μ_n, k_t, μ_t, α, β. A methodology has to be developed in order to determine automatically:

- the model parameters as functions of the physical constants of the contacting surfaces such as the Young's modulus and the Poisson's ratio.

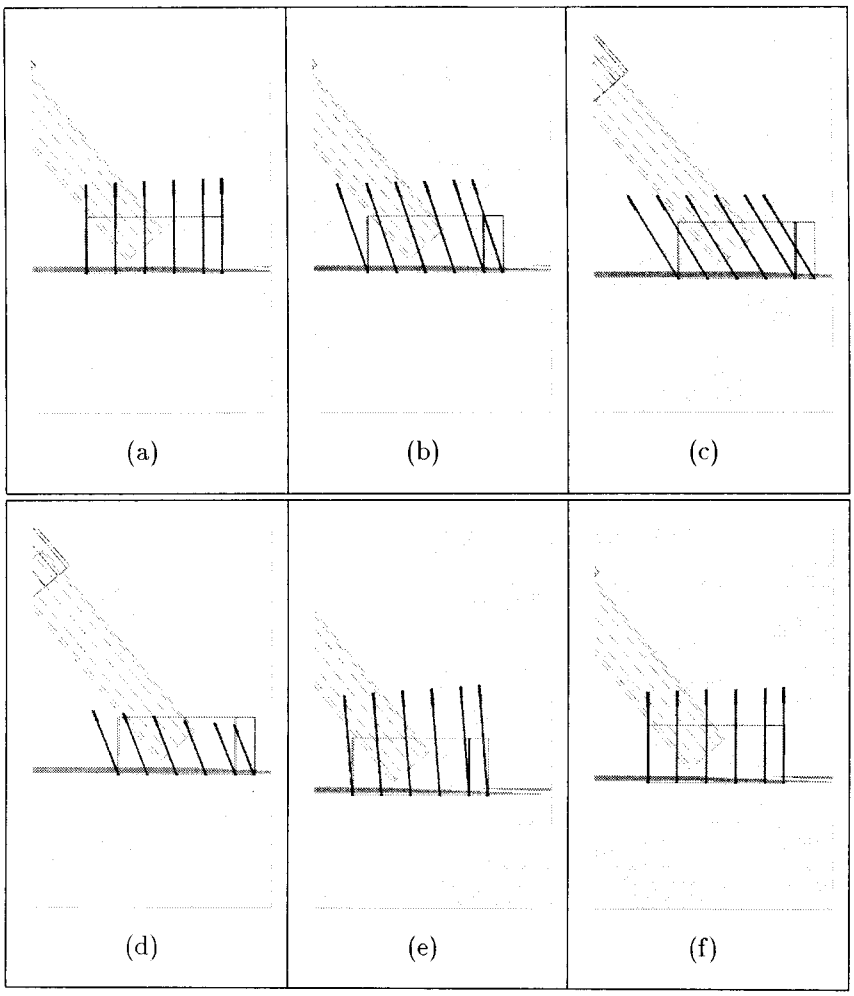

Fig. 19. Contact forces during the sliding simulation.

https://doi.org/10.1017/S0263574799001290 Published online by Cambridge University Press

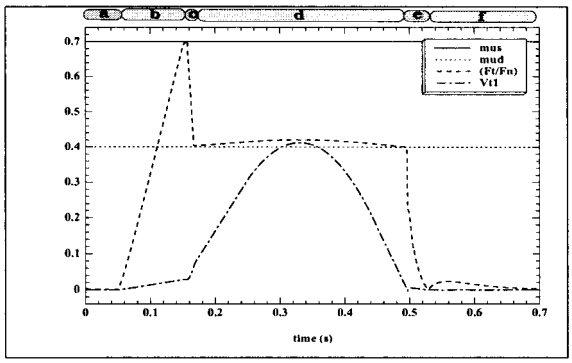

Fig. 20. Evolution of the ratio λ_g and the sliding velocity.

- the number N of testing points required to obtain smooth curves for normal and tangential forces during support phase as close as possible to the standard recorded ground reaction.
- the number N of testing points and their distribution as functions of the size of the ground irregularities.

5. CONCLUSIONS

After a discussion about the two main approaches used to simulate the foot/ground interaction, we have explained our choice of the spring-damper model, mainly in order to simulate ground compliance. Then we have shown the necessity to use distributed force contact model rather than a unique contact force model. We have presented a complete model that incorporates all macroscopic phenomena that may occur during the locomotion cycle: impact, transition from impact to contact, contact during support with static friction, transition from static friction to sliding friction, sliding friction. Finally we have discussed the obtained results for an anthropomorphic walking biped robot. We have underlined the deficiencies of the model and namely raised the necessity of a methodology to determine accurately the values of the model parameters as functions of the physical constants of the contacting surfaces and to determine the ideal number of testing points required.

References

1. W. Blajer and W. Schiehlen, "Walking without impacts as a motion/force control problem", *J. Dynamic Systems, Measurement, and Control* **114**, 660–665 (Decembr, 1992).
2. A.M. Formal'sky, "Impulsive control for anthropomorphic biped", *Theory and Practice of Robots and Manipulators, Proceeding sof RoManSy'94* (1994) pp. 387–393..
3. F.B. Ouezdou, "Outils d'Aide à la Conception de robots à locomotion articulée", *Thèse de Doctorat* (l'Université Pierre et Marie Curie, 1990).
4. Y.-J. Seo and Y.-S. Yoon, "Design of a robust dynamic gait of the biped using the concept of dynamic stability margin, *Robotica* **13**, Part 4, 461–468 (1995).
5. J.J. Moreau, "Unilateral contact and dry friction in finite freedom dynamics", In: *Non-smooth Mechanics and Applications* (ed. by J.J. Moreau and P.D. Panagiotopoulos) Wien (1988) pp. 1–82.
6. D. Baraff, "Fast Contact force computation for non penetrating rigid bodies", *SIG-GRAPH*, Orlando (July 24–29, 1994) pp. 23–34.
7. F. Pfeiffer and C. Glocker, *Multibody Dynamics with Unilateral Contacts* (Wiley Series in Nonlinear Science, New York, 1996).
8. F. Génot, B. Brogliato, R.M. Brach and B. Thuilot, "On LCPs and tangential impacts in rigid body mechanics with unilateral constraints and dry friction", *Proceeding of the fifth IFAC Symposium on Robot Control*, Nantes (September 3–5, 1997) pp. 861–868.
9. P.S. Freeman and D.E. Orin, "Efficient dynamic simulation of a quadruped using a decoupled tree-structure approach", *Int. J. Robotics Research* **10**, No. 6, 619–627 (1991).
10. M. Raibert, *Legged Robots that Balance* (MIT Press, Cambridge, Mass., 1986).
11. F. Plas, E. Viel and Y. Blanc, "*La Marche Humaine, Kinésiologie Dynamique, Biomécanique et Pathomécanique* (Masson, Paris, 1989).
12. M. Vukobratovic, B. Borovac, D. Surla and D. Stokic, "*Biped Locomotion*, **Vol. 7** of *Scientific Fundamentals of Robotics* (Springer-Verlag, Berlin, 1990).
13. D.W. Marhefka and D.E. Orin, "Simulation of contact using a nonlinear damping model", *IEEE Proceeding of Int. Conf. on Robotics and Automation* (1996) pp. 1662–1668.
14. W. Goldsmith, *Impact, the Theory and Physical Behavior of Colliding Solids* (Edward Arnold, London, 1960).
15. K.H. Hunt and F.R.E. Crossley, "Coefficient of restitution interpreted as damping vibroimpact", *Transactions of the ASME* 440–445 (1975).
16. C. Canudas de Wit, H. Olsson, K.J. Åstròm and P. Lischinsky, "A new model for control of systems with friction", *IEEE Transactions on Automatic Control* **40**, No. 3, 419–425 (1995).
17. B. Armstrong, "Stick-slip arising from stribeck friction", *IEEE Int. Conf. on Robotics and Automation* Cincinnati (1990) pp. 1377–1382.
18. C. Tzafestas and P. Coiffet, "Real-Time collision detection using spherical octrees: virtual reality application", *IEEE Int. Workshop on Robot and Human Communication, RO-MAN' 1996*, Tsukuba (1996) pp. 500–506.
19. E.P. Hanavan, "A mathematical model of the human body", *AMRL-TR, 64–102* (Aero Medical Research Laboratories. Wright Patterson, A.F. Base, OHIO, 1964).
20. A.A. Grishin, A.M. Formal'sky, A.V. Lensky and S.V. Zhitomirsky, "Dynamic walking of two biped vehicles", *IFToMM Proceedings of the Ninth World Congress on the Theory of Machines and Mechanisms*, Italy (1995) pp. 2308–2312.

https://doi.org/10.1017/S0263574799001290 Published online by Cambridge University Press